Thermal Science and Engineering (2022) Volume 5 Issue 2
doi:10.24294/tse.v5i2.1534

CASE REPORT

Analysis of coupling characteristics between solar energy and compressor extraction energy storage gas turbine CHP system

Hailiang Yang, Cheng Yang*, Guangping Xie, Hua Li, Xiaoqian Ma

School of Electric Power, South China University of Technology, Guangzhou 510640, Guangdong province, China. E-mail: chyang1@scut.edu.cn

ABSTRACT

The regulation of compressor extraction and energy storage can improve the performance of gas turbine energy system. In order to make the gas turbine system match the external load more flexibly and efficiently, a gas turbine cogeneration system with solar energy coupling compressor outlet extraction and energy storage is proposed. By establishing the variable condition mathematical model of air turbine, waste heat boiler and solar collector, we use Thermoflex software to establish the variable condition model of gas turbine compressor outlet extraction, and analyze the variable condition of the coupling system to study the changes of thermal parameters of the system in the energy storage, energy release and operation cycle. Taking the hourly load of a hotel in South China as an example, this paper analyzes the case of the cogeneration system of solar energy coupling compressor outlet extraction and energy storage, and compares it with the benchmark cogeneration system. The results show that taking a typical day as a cycle, the primary energy utilization rate of the system designed in this paper is 3.2% higher than that of the traditional cogeneration system, and the efficiency is 2.4% higher.

Keywords: Cogeneration; Gas Turbine; Pumping Energy Storage; Solar Energy; Off Design Characteristics

ARTICLE INFO

Received: 6 Jane 2022
Accepted: 2 August 2022
Available online: 7 August 2022

1. Introduction

With the proposal of the national strategic goal of carbon peak and carbon neutrality, the transformation of low-carbon energy in China is imperative. Large scale consumption of new energy will become the basic trend of "energy revolution". In order to improve the stability and security of power system, it is of great significance to improve the flexibility and efficiency of gas turbine system[1].

The combined heat and power (CHP) system of gas turbine generates steam by recovering the low-grade waste heat in the exhaust gas of gas turbine, and sends it to the end users for heating through the pipe network. Through the cascade utilization of energy, the energy utilization rate of the system is greatly improved[2]. Compared with the power generation efficiency of gas turbine (generally not higher than 40%), the comprehensive energy utilization rate of CHP system can reach 90% at most[3,4]. In order to make it adapt to the fluctuation of external load, how to keep the unit efficiently and flexibly adapt to the external load is one of the important contents that the current CHP system needs to study. Yang *et al.*[5] takes 390 MW pumped condensing cogeneration unit as the research object, and determines the system energy supply condition and peak shaving depth, which has guiding significance for the economic and efficient operation of the unit. Xu *et al.*[6] used

Ebsilon simulation software to establish the model of cogeneration unit to calculate the variable conditions of pure condensing and extraction conditions.

In order to enhance the source charge coupling characteristics of CHP system, energy storage and renewable energy can be considered. Yang *et al.*[7] proposed a gas turbine system using compressor outlet extraction to store energy, and analyzed the source load coupling characteristics of the system under different step loads. However, there is heat loss in the air storage room and the air parameters at the inlet of the air turbine are low. Solar energy can be considered to heat the air at the inlet of the air turbine to improve the power generation efficiency of the system. Solar energy is widely used in the field of power generation because of its clean and cheap characteristics. However, due to the instability of solar energy, it generally only plays the role of auxiliary heating[8,9]. Yang *et al.*[10] proposed a gas turbine cogeneration system with solar energy coupled with compressed air energy storage, and analyzed the source load coupling performance of the system. The results show that the system with solar assisted heating has higher efficiency.

The existing literature studies the variation performance of the system itself, and rarely discusses the problem of matching the hourly load between the system and the outside world. In order to make the CHP system have good coupling characteristics of source and load, this paper proposes a CHP system with solar energy coupling compressor outlet extraction and energy storage. While studying the variation performance of the system, it also analyzes the coupling characteristics of the system and the hourly load of the outside world. Aiming at the hourly load of a hotel in South China, it analyzes the advantages of the designed system compared with the traditional cogeneration system.

2. System description

2.1 System operation mode

Figure 1 shows the CHP system of a gas turbine with solar energy coupled compressor extraction and energy storage. It can be seen from **Figure 1** that the system is composed of CHP system, solar energy collection system and air extraction energy storage/release system. CHP system is composed of a compressor, a combustion chamber, a gas turbine, a generator and a waste heat boiler. The solar energy collection system is composed of a trough solar mirror field, a pump, a heat transfer oil, a high and low temperature heat storage tank and an oil-gas heat exchanger. The air extraction and energy storage/release system are composed of the last stage air extraction pipeline of the compressor, the constant pressure air extraction valve, the constant pressure adiabatic air storage chamber, the constant pressure air release valve, the oil-gas heat exchanger, the air turbine and the generator.

When the power generation of the gas turbine is greater than the external load demand, the system enters the energy storage stage. At this time, the exhaust valve at the outlet of the compressor is opened to realize the load reduction operation of the gas turbine through air extraction. The extracted high-temperature and high-pressure air enters the water gas heat exchanger to heat the water supply, so as to produce steam for heating. The cooled air is stored in the constant pressure adiabatic air storage chamber.

In addition, the trough mirror field collects the heat transfer oil in the solar radiation heating circuit, and its flow is adjusted according to the fluctuation of solar radiation intensity. After it is heated to the specified temperature, it is stored in the high-temperature heat storage tank.

When the power generation of gas turbine is less than the external load demand, the system enters the energy release stage. At this time, the constant pressure relief valve is opened, and the high-pressure air enters the air turbine to expand and do work after being heated by the oil-gas heat exchanger, driving the generator to generate electricity to make up for the power supply gap. In addition, the heat transfer oil in the high-temperature heat storage tank is pumped to the heat exchanger for heat exchange with the low-temperature air. Its flow is determined by the air temperature at the inlet of the air turbine. The cooled low-temperature heat transfer oil enters the low-temperature heat storage tank.

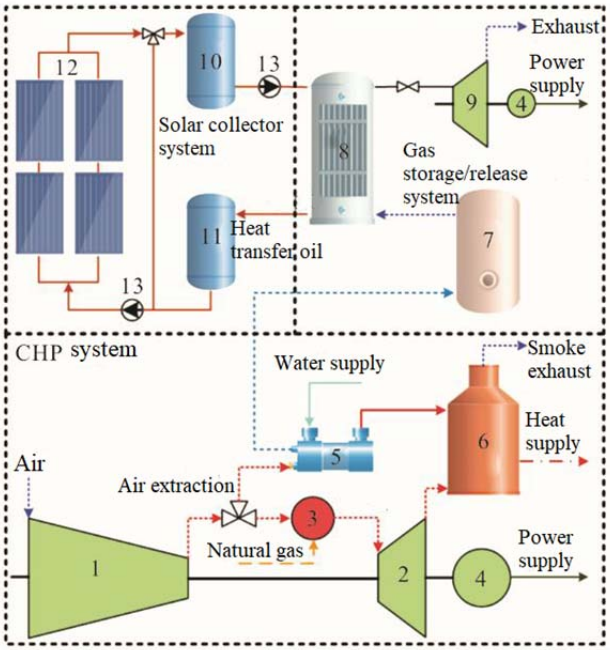

Figure 1. Schematic diagram of the system flow chart**.** 1—compressor; 2—gas turbine; 3—combustion chamber; 4—generator; 5—water gas heat exchanger; 6—waste heat boiler; 7—gas storage room; 8—oil gas heat exchanger; 9—air turbine; 10—high temperature heat storage tank; 11—low temperature heat storage tank; 12—solar collector; 13—heat transfer oil pump.

2.2 system model

2.2.1 Models of components of cogeneration system

In this paper, Thermoflex thermal simulation software is used to establish the variation model of gas turbine extraction, and the inlet flow of the compressor remains unchanged during the extraction load reduction process.

Large axial-flow gas turbines mainly rely on changing the opening of compressor inlet guide vane (IGV) to adjust power. When the IGV opening increases from 0 to 100%, the air flow increases from 70% of the rated value to 100%. The small gas turbine studied in this paper can be regarded as the IGV opening remains the largest, and the compressor outlet extraction replaces the IGV function. In view of the fact that excessive air extraction may lead to unstable combustion conditions, the extraction coefficient α (the ratio of compressor extraction mass flow to intake mass flow) to be studied in this paper is taken as 0–0.25.

The efficiency of waste heat boiler is closely related to the exhaust gas parameters of gas turbine. The following model can be used to calculate the vatiation performance of waste heat boiler[11]:

$$\beta = \frac{Q_{\mathrm{HRSG}}}{Q_{\mathrm{HRSG\,0}}} \tag{1}$$

$$\eta = \eta_0 \left(0.0951 + 1.525\beta - 0.6249\beta^2\right) \tag{2}$$

Where: Q_{HRSG} and Q_{HRSG0} respectively represent the actual thermal load and design thermal load of waste heat boiler, kW; β indicates the load rate of waste heat boiler; η and η_0 refers to the actual thermal efficiency and design thermal efficiency of waste heat boiler respectively.

2.2.2 Component models of solar energy-air extraction energy storage/release system

The variable condition model of the air turbine can be determined with the following formula[12]:

$$\bar{m} = \sqrt{\frac{T_0}{T}\sqrt{\frac{\pi^2 - 1}{\pi_0^2 - 1}}} \tag{3}$$

$$\bar{\eta} = \left[1 - 0.3(1 - \dot{n})^2\right]\left(\frac{\dot{n}}{\dot{m}}\right)\left(2 - \frac{\dot{n}}{\dot{m}}\right) \tag{4}$$

Where: T is the turbine inlet temperature, K; π is the expansion ratio; $\bar{m}$ is the ratio of turbine inlet mass flow to design value; m is the turbine intake mass flow, kg/s; η is the isentropic expansion efficiency of air turbine; $\bar{\eta}$ is the ratio of isentropic expansion efficiency of air turbine to design value; n is the speed, r/min; subscript 0 indicates the design value; superscript $\dot{}$ indicates the ratio of operating converted parameters to rated converted parameters.

Trough solar collector is selected, and the medium in the circuit is Thermol VP-1 heat transfer oil. This paper adopts the following calculation model of trough solar collector[13]:

$$Q_{\mathrm{s}} = N \cdot A \cdot D_{\mathrm{DNI}} \tag{5}$$

$$Q_{\mathrm{a}} = \eta_{\mathrm{s}} \cdot Q_{\mathrm{s}} \tag{6}$$

Where: Q_{s} and Q_{a} represent the heat projected onto the surface of the collector and the actual heat absorbed by the collector; N refers to the number of collector plates; A represents the area of a single collector plate, m^2; D_{DNI} refers to solar radiation

intensity, W/m^2; η_s indicates collector efficiency[14].

$$\eta_s = 73.3k(\theta) - 0.01(T_{io} - T_a)(0.727\ 6 - \frac{4.96}{D_{DNI}} - 6.91 \cdot \frac{T_{io} - T_a}{D_{DNI}}) \tag{7}$$

Where: $K(\theta)$ is the correction coefficient of incident angle; T_a is the average ambient temperature, 293.15 K; T_{io} is the average temperature of the inlet and outlet of the heat conducting fluid, K.

The calculation formula of $K(\theta)$ is[15]:

$$K(\theta) = \cos(\theta) - 3.512 \times 10^{-4}\theta - 3.137 \times 10^{-4}\theta^2 \tag{8}$$

Where: θ is the angle of incidence. The calculation formula is[16]:

$$\cos(\theta) = \sqrt{\cos^2(\theta_z) + \cos^2(\delta) \cdot \sin^2(\omega)} \tag{9}$$

Where: θ_z, δ and ω are zenith angle, declination angle and solar hour angle respectively. The calculation method of θ_z, δ and ω is:

$$\delta = 23.45 \cdot \sin\left(2\pi \frac{284 + n}{365}\right) \tag{10}$$

$$\cos(\theta_z) = \sin(\phi) \cdot \sin(\delta) + \cos(\phi) \cdot \cos(\delta) \cdot \cos(\omega) \tag{11}$$

$$\omega = 15 \cdot (t_h - 12) \tag{12}$$

Where: n is the date serial number, and January 1 of each year is the first day; ϕ is the local latitude, 23.1°; t_h is the moment.

Similar to literature of Zhao[17], the analytical formula of pump head and efficiency is:

$$\dot{H} = 1 - 6.965 \times 10^{-3}\dot{Q}^{1.555\ 8} + 5.949\ 2 \times 10^{-5}\dot{Q}^{3.111\ 6} - 1.043\ 2 \times 10^{-5}\dot{Q}^{4.667\ 4} \tag{13}$$

$$\dot{\eta} = -0.257\ 84 + 1.080\ 52\dot{Q}^{0.6} + 5.252 \times 10^{-2}\dot{Q}^{1.2} - 4.608 \times 10^{-2}\dot{Q}^{1.8} \tag{14}$$

Where: H refers to pump head, m; Q refers to heat transfer oil flow, L/s; η_p is the total efficiency of the pump; superscript $\dot{}$ indicates the ratio to the design value.

The calculation of the heat exchanger adopts the effective heat transfer unit number method. During the operation, the inlet and outlet temperature of the heat transfer oil side remains unchanged. the inlet flow of the heat transfer oil and the outlet temperature of the air are ajusted.

The following assumptions are made for the gas storage chamber/heat storage tank: 1) the gas/liquid constant pressure at the outlet of the gas storage chamber/heat storage tank does not change with the indoor gas/liquid quality; 2) the air chamber/heat storage tank is insulated, i.e. there is no heat loss.

3. System performance evaluation index and parameter design

3.1 System performance evaluation index

3.1.1 CCHP system

The primary energy utilization rate η_{th} is:

$$\eta_{th} = \frac{P_e + Q_h}{P_f} \times 100\% \tag{15}$$

Exergy efficiency η_{ex} is:

$$\eta_{ex} = \frac{E_e + E_h}{E_f} \times 100\% \tag{16}$$

3.1.2 Solar energy coupled gas storage room storage/release system

The solar power P_s is:

$$P_s = P_a - P_{a0} \tag{17}$$

Net power P_a of air turbine is:

$$P_a = P_T - P_P \tag{18}$$

Solar energy contribution ε is:

$$\varepsilon = \frac{P_s}{P_a} \times 100\% \tag{19}$$

3.1.3 Coupling system

The primary energy utilization rate η_t is:

$$\eta_t = \frac{P_a + P_e + Q_h}{P_a + Q_s} \times 100\% \tag{20}$$

Exergy efficiency $\eta_{ex\text{-}s}$ is:

$$\eta_{ex\text{-}s} = \frac{E_e + E_h}{E_f + E_s} \tag{21}$$

Where: P_e, Q_h, P_f respectively represents the power of gas turbine, heating capacity and the en-

ergy of fuel input system, kW; P_{a0}, P_t, P_p respectively represents the net power of air turbine before solar heating, the power of upper turbine and the non power consumption of heat transfer oil, kW; E_e, E_h, E_f, E_{solar} are electricity, heat, fuel and input solar energy respectively.

$$E_e = P_e + P_a \tag{22}$$

$$E_h = Q_e\left(1-\frac{T_o}{T_h}\right) \tag{23}$$

$$E_f = P_f \tag{24}$$

$$E_{solar} = m_{oil}\left[c_p\left(T_{oil} - T_{oil\text{-}in}\right) - T_o c_p \ln\frac{T_{oil}}{T_{oil\text{-}in}}\right] \tag{25}$$

Where: T_o, T_h, T_{oil}, $T_{oil\text{-}in}$ respectively represents the reference temperature, heating steam temperature, heat transfer oil temperature at the collector outlet and heat transfer oil flow at the collector inlet, K; m_{oil} represents the mass flow of heat transfer oil, kg/s; c_p represents the average specific heat capacity of heat transfer oil, kJ/(kg·K).

Table 1. Simulation values of the main design parameters of gas turbine

Object	Stimulation value	Design value	Relative error/%
Ambient temperature/°C	15	15	0
Generating power/kW	4,753	4,821	-1.43
Pressure ratio	13.97	14.05	-0.57
Compressor efficiency	0.88	0.88	0
Compressor outlet temperature/°C	19.18	19.18	0
Intake air flow/(kg·s^{-1})	509.1	511.4	-0.45
Turbine exhaust temperature/°C	1,100	1,100	0
Turbine inlet temperature/°C	0.317	0.314	0.95
Fuel flow/(kg·s^{-1})	384.6	388.3	-1.39
Net efficiency	0.300	0.307	-2.33

3.2 System design parameters

CHP system is composed of small gas turbine, waste heat boiler and other components. Thermoflex thermal simulation software is used to establish the gas turbine exhaust variable condition model, and the calculated value of the mathematical model is used to verify the simulated value of Thermoflex software. The results are shown in **Table 1**. It can be seen from **Table 1** that the ror between the simulated value and the design

Table 2. Design parameters of other main components

Object		Numerical value
Waste heat boiler	Efficiency	0.8
	Smoke exhaust temperature/°C	87.0
	Steam pressure/MPa	0.9
	Steam temperature/°C	175.0
Air turbine	Inlet air temperature/°C	390
	Inlet air pressure/MPa	1.069
	Power generation efficiency	0.880
	Air temperature at the outlet of air tank/°C	190
	Turbine exhaust pressure/MPa	0.103
Solar collector	Collector length/m	150.00
	Collector width/m	5.76
	Temperature of heat transfer oil entering and leaving the collector/°C	221.19/ 400.00
	Number of collectors	10
	Date serial number	152
	Time	12
	Local latitude/(°)	23.1
	Ambient temperature/°C	20
	Solar radiation intensity/(W·m^{-2})	800
	Illumination time/h	5
	Volume of high temperature heat storage tank /m^3	172.29
	Volume of low temperature heat storage tank /m^3	152.62
Oil-air heat exchanger	Air flow/(kg·s^{-1})	2.4
	Heat transfer oil flow/(kg·s^{-1})	1.2
	Heat exchange area/m^2	21.8
	Heat exchange coefficient/(W·(m^2·K)$^{-1}$)	1,221.1

value of each parameter of the gas turbine is within 3%.

All the high-temperature flue gas charged by the gas turbine enters the waste heat boiler to heat the waste heat boiler feed water and generate superheated steam, which can heat or drive the LiBr absorption refrigerator. The design parameters of waste heat boiler, air turbine, solar collector and oil air heat exchanger are shown in **Table 2**.

4. Analysis of system variety-duty condition

4.1 Gas turbine variety-duty condition analysis

Figure 2 shows the influence of compressor outlet extraction on important parameters of gas turbine. It can be seen from **Figure 2** that the pressure ratio and outlet temperature of the compressor, the power and efficiency of the gas turbine decrease with the increase of the extraction coefficient, the extraction coefficient increases from 0 to 0.25, and the efficiency of the gas turbine decreases from 30% to 14.4%. There are two reasons for the decrease of pressure ratio: (1) the extraction pipeline at the outlet of the compressor leads to the increase of the overall flow section of air/gas; (2) the exhaust gas from the compressor outlet causes the gas turbine to work at part load, the flow into the combustion chamber and the gas turbine is reduced, and the flow resistance of the combustion chamber and the exhaust section of the gas turbine is reduced[5]. As the pressure ratio decreases, the temperature ratio at the inlet and outlet of the compressor also decreases, and the temperature at the inlet of the compressor changes little, so the temperature at the outlet of the compressor decreases.

The exhaust of the compressor outlet will reduce the air entering the combustion chamber, the exhaust flow of the gas turbine and the heat absorption of the waste heat boiler. The influence of extraction coefficient on the efficiency and heat supply of waste heat boiler is shown in **Figure 3**. As can be seen from **Figure 3**, the exhaust coefficient increases, and the efficiency and heating capacity of the waste heat boiler decreases.

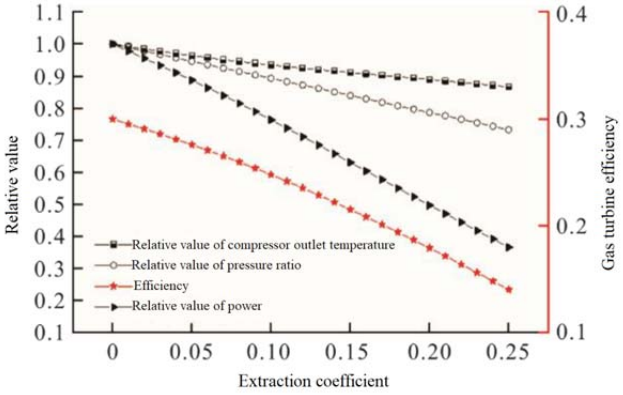

Figure 2. Effect of air extraction ratio on pressure ratio, gas turbine output power, gas turbine efficiency, and air extraction temperature.

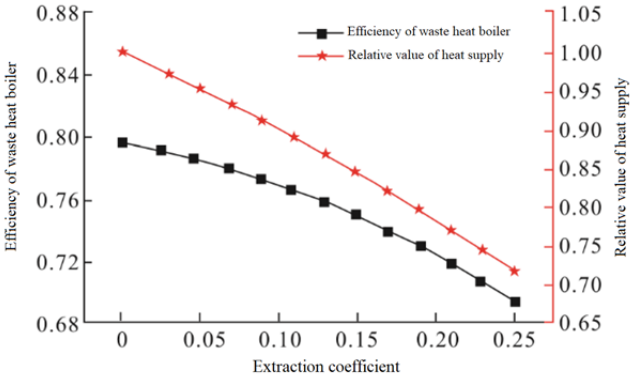

Figure 3. Effect of air extraction ratio on the efficiency and heat output of the heat recovery steam generator.

4.2 Analysis of variety-duty conditions of solar energy extraction storage/release energy system

The power generation and efficiency of the air turbine are determined by the air parameters at the inlet. Usually, the temperature and flow of the air at the inlet of the turbine can be adjusted to control the power of the air turbine. Temperature regulation can be achieved by changing the flow of heat transfer oil in the oil-air heat exchanger, and flow regulation can be achieved by changing the opening of the constant pressure relief valve. **Figure 4** shows the influence of air flow and temperature on the turbine. As can be seen from **Figure 4**: with the temperature unchanged, the smaller the air flow, the lower the power generation of the turbine. With the reduction of the air flow at the turbine inlet, the reduction rate of the turbine power generation is faster and faster; when the air flow is constant, the power generation of the air turbine decreases with the decrease of temperature; when the air flow drops below 50% of the design value, the air turbine

stops working.

The heat transfer oil in the low-temperature heat storage tank is heated to the set temperature by the trough solar collector. The variation curve of heat transfer oil mass flow and heat transfer oil pump power consumption with solar radiation intensity is shown in **Figure 5**.

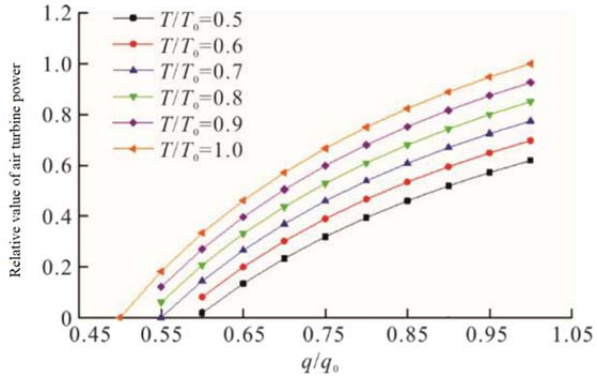

Figure 4. Effect of air turbine inlet air temperature and flow rate on turbine output**.**

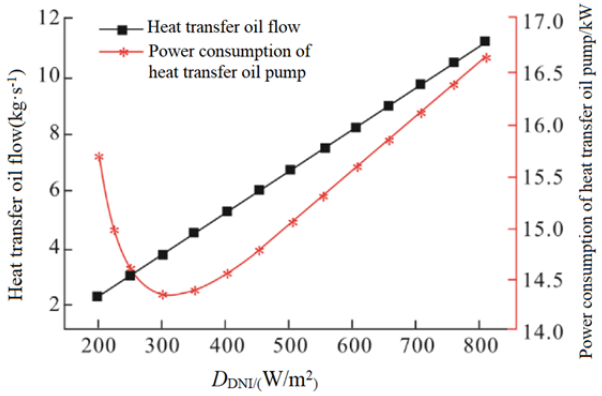

Figure 5. Variation curves of heat transfer oil mass flow rate and power consumption of oil pump with solar radiation intensity**.**

It can be seen from **Figure 5** that with the increase of solar radiation intensity, the flow of heat transfer oil and the efficiency of centrifugal pump increase, and the power consumption of heat transfer oil pump first decreases and then increases. When the solar radiation is 325 W/m^2, the power of heat transfer oil pump is the smallest.

The heat exchange between solar energy and air is controlled by the flow of heat transfer oil at the outlet of high-temperature heat storage tank. The air temperature at the inlet of the oil-air heat exchanger is constant at 190 ℃, and the pressure is 1.069 MPa. According to the external demand, the heat transfer oil heats the air to different temperatures. However, due to the limitation of the temperature of the heat transfer oil, the maximum temperature of the air at the outlet of the heat exchanger is 382.4 ℃. Solar energy contribution represents the ratio of solar power generation power to turbine power. The greater the solar energy contribution, the greater the impact of solar energy on turbine power. The solar energy contribution under different turbine inlet parameters is shown in **Figure 6**. It can be seen from **Figure 6** that when the air flow is constant, the higher the turbine inlet temperature is, the greater the solar energy contribution is. When the temperature is constant, the smaller the flow is, the greater the solar energy contribution is.

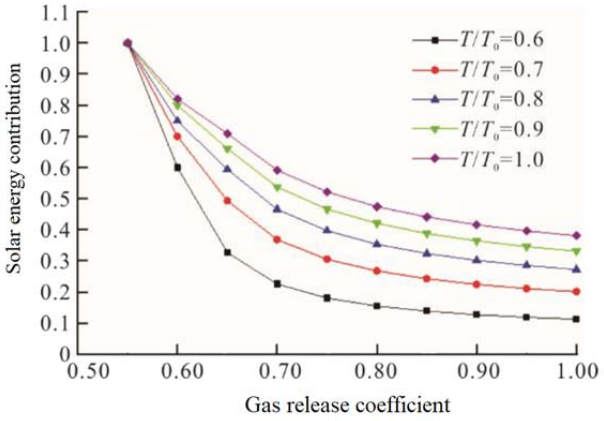

Figure 6. The solar contribution degrees with different turbine inlet parameters**.**

4.3 Analysis of variable working conditions of coupling system

The gas storage and release conditions of the system are not synchronized, which is determined by the external demand power and the power of the gas turbine. The variety-duty condition of the coupling system is divided into two stages: pumping and energy storage stage and energy release stage.

(1) Energy storage stage. When the external demand power is lower than the rated power of the gas turbine, the compressor outlet exhausts air to regulate the power of the gas turbine, and the extracted gas is cooled and stored in the gas storage chamber. The change of the primary energy utilization and efficiency of the system with the extraction coefficient during energy storage is shown in **Figure 7**. As can be seen from **Figure 7**, as the extraction coefficient increases, the primary energy utilization and efficiency of the system decrease faster and faster. It can be seen that although the extrac-

tion can realize the flexible peak shaving of gas turbine, the efficiency is seriously decreased.

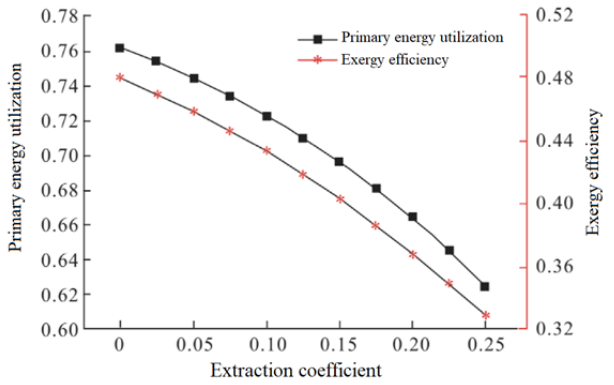

Figure 7. Variations of the primary energy utilization ratio and exergy efficiency with air extraction ratio during energy storage.

(2) Gas release stage. When the external electric power demand is greater than the power of the gas turbine, the air turbine is put into operation to increase the system power. Define the gas release coefficient r, which represents the ratio of the actual gas release flow of the gas storage chamber to the gas release flow under the design condition, $r=q/q_0$. The larger the r, the larger the air turbine inlet flow is. The changes of the primary energy utilization and exergy efficiency of the system with the gas release coefficient during energy release are shown in **Figure 8**. It can be seen from **Figure 8** that with the increase of gas release coefficient, the primary energy utilization rate and efficiency of the system increase. The analysis shows that the efficiency of the air turbine increases with the increase of the air release flow, and the more solar energy is used, the higher the efficiency of the system.

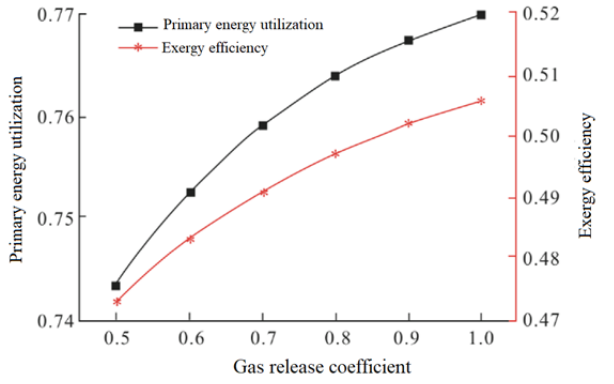

Figure 8. Variations of the primary energy utilization ratio and exergy efficiency with air release ratio during energy release.

The unit performance and air extraction volume in one cycle are related to the air extraction/release time. Define the parameter extraction/release time ratio $h=T_c/T_s$. T_c and T_s represent the extraction energy storage time and release time h respectively. The larger the h is, the more gas is stored in one cycle.

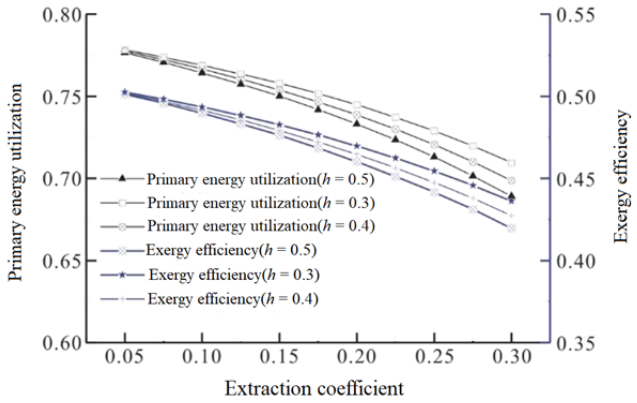

Figure 9. Variations of the primary energy utilization ratio and exergy efficiency of the system in a period.

Assuming that the gas storage volume is equal to the gas release volume in one cycle, and the gas release speed and extraction speed are constant, the changes in the primary energy utilization and efficiency of the system are shown in **Figure 9**. It can be seen from **Figure 9** that in one cycle, h remains unchanged, and the primary energy utilization rate and exergy efficiency of the system decrease with the increase of the extraction coefficient. The efficiency of the system decreases significantly when pumping and storing energy. The larger the pumping coefficient, and the longer the time, the lower the primary energy utilization and exergy efficiency.

5. Case analysis

5.1 Load distribution

Taking a hotel building[18] in South China as an example, the hourly load (including electrical load, cooling load and heating load) of the building on a typical day is analyzed. Since the absorption refrigerator is driven by steam, the cooling load is converted into the heating load for the convenience of research.

The changes of solar radiation intensity and ambient temperature with time are shown in **Figure 10**. It can be seen from **Figure 10** that there is solar radiation between 6:00 and 19:00, and the solar radiation is the largest at 13:00. The peak value of the temperature in a day occurs at 15:00, and the tem-

perature in a day is greater than 20 ℃.

The typical daily electrical load and thermal load distribution are shown in **Figure 11**. It can be seen from **Figure 11** that the peak period of electricity and heat consumption in a day is from 11:00 to 17:00, and the electrical load reaches the maximum at 11:00, and the thermal load reaches the peak at 18:00.

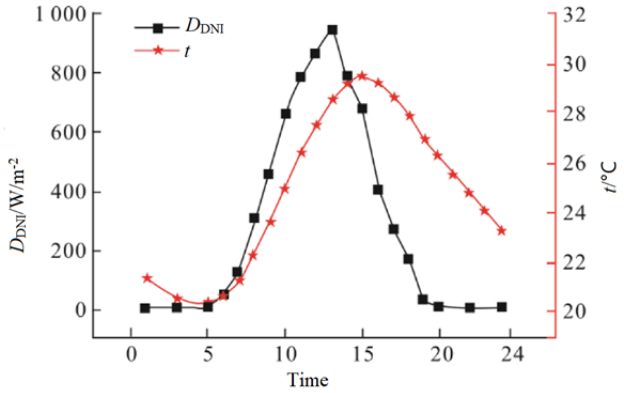

Figure 10. Variations of the solar radiation intensity and ambient temperature with time.

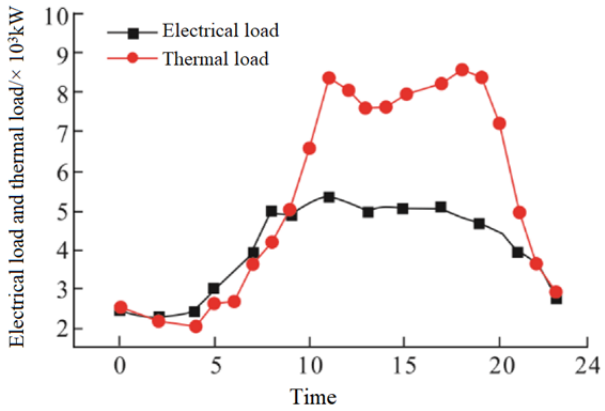

Figure 11. Distribution of the electrical load and thermal load in a typical day.

5.2 Baseline CHP system description

Table 3. Main design parameters of the gas turbine in the benchamark system

Project	Design value
Ambient temperature/°C	15
Generating power/kW	5,354
Pressure ratio	14.15
Compressor efficiency	0.88
Compressor outlet temperature/°C	385.7
Intake air flow/(kg·s^{-1})	19.53
Turbine exhaust temperature/°C	519.1
Turbine inlet temperature/°C	1,110
Fuel flow/(kg·s^{-1})	0.344
Net efficiency	0.302

In order to reflect the advantages of the design system, the design system is compared with the benchmark system. The reference system is not equipped with compressor outlet extraction, and the gas turbine works between no-load and full load by adjusting the inlet air flow and fuel flow, so as to meet the needs of external electrical load. The specific design parameters of the reference system are shown in **Table 3**, and the design parameters of the waste heat boiler are the same as those in **Table 2**.

5.3 Coupling calculation between the system and the outside world

The system adopts the operation mode of "determining heat by electricity". The excess heat is stored in the thermal storage tank (TED). When the heat is insufficient, the heat in the thermal storage tank is preferred for heating. When the heat in the thermal storage tank is insufficient, the peak boiler is added for heating; if the power is insufficient, you can buy it from the outside, and the excess power can be connected to the Internet. The variation of system air release coefficient and extraction coefficient with time in one cycle is shown in **Figure 12**.

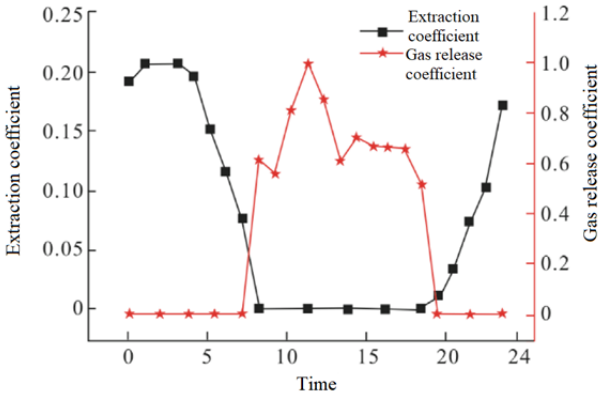

Figure 12. Variations of the air release and extraction ratio with time.

It can be seen from **Figure 12** that the system is in the gas release stage from 8:00 to 19:00, and the gas release coefficient is the largest; the rest of the time is in the stage of gas extraction and energy storage, and the gas release coefficient is the largest at 11:00; 1:00–3:00 the external electrical load is the lowest, and the compressor extraction coefficient is the largest.

The efficiency of the system has been improved due to the addition of energy storage and the introduction of solar energy. **Table 4** shows the comparison between the design system and the benchmark system. It can be seen from **Table 4**

that although the design system consumes 5.2% more natural gas than the benchmark system, the primary energy utilization rate has increased by 3.2%, the efficiency has increased by 2.4%, and there is still remaining heat of 1.5×10^5 MJ that can be used for the next cycle.

Table 4. Comparison between the design system and the benchmark system

Project	Design system	Benchmark system
Total power output/MW	3.493×10^5	3.493×10^5
Total heat output/MJ	6.088×10^5	4.618×10^5
Residual heat/MJ	1.5×10^5	30.75
Fuel consumption/kg	24,410.41	25,748.35
Solar energy input heat/MJ	1.4×10^4	
Gas turbine efficiency	0.261	0.298
Primary energy utilization	0.724	0.692
Exergy efficiency	0.451	0.427

6. Conclusion

In this paper, a CHP system with solar energy coupling compressor extraction and energy storage is proposed. The components and systems are analyzed under variable working conditions, and the advantages of designing the system under hourly load are studied. The main conclusions are as follows.

(1) The exhaust gas from the compressor outlet leads to the reduction of the efficiency of the gas turbine and the efficiency of the waste heat boiler. When the maximum extraction coefficient is 0.25, the efficiency of gas turbine and waste heat boiler are 16.2% and 11.7% lower than the design value.

(2) The smaller the air flow and temperature at the inlet of the air turbine, the lower the power and efficiency of the air turbine; when the air flow at the inlet of the air turbine is less than 50% of the design value, the air turbine will stop working; the smaller the air flow at the inlet of the air turbine, the higher the inlet temperature, and the greater the contribution of solar energy.

(3) Taking the hourly load of a building in South China as an example, the air extraction coefficient and air release coefficient of the designed system and the traditional cogeneration system are compared at different times. The results show that although the design system consumes 5.2% more natural gas than the benchmark system, the primary energy utilization rate of the design system is 3.2% higher than that of the traditional cogeneration system, and the efficiency is 2.4%.

References

1. Gao C, Xiao B, Yin H, *et al*. Energy storage participating in thermal power peaking and configuration in background of new energy: A review. Thermal Power Generation 2019; 48(10): 38–43.
2. Ma D. Introduction of distributed energy supply cogeneration system of cooling, heating and electrics. Inner Mongolia Electric Power 2011; 29(1): 9–10.
3. Wang T, Song W. Discussion on the technologies of combined cooling, heating and power. Applied Energy Technology 2010; (3): 35–38.
4. Zhu J, Shi L. Application and development of gas CCHP system. Huadian Technology 2014; 36(10): 73–76, 80.
5. Yang C, Liu H, Wang P, *et al*. Economic analysis on peak-regulation of GTCC cogeneration unit with extraction heating. Proceedings of the CSEE 2020; 40(2): 592–601.
6. Xu K, Li W, Li M, *et al*. Analysis on heat supply performance of gas-steam combined cycle cogeneration units. Thermal Power Generation 2019; 48(5): 1–7.
7. Yang C, Huang M, Wang P, *et al*. Analysis on improving flexibility of a gas turbine-based energy system with compressor bypass air extraction for energy storage. Proceedings of the CSEE 2018; 38(18): 5510–5517.
8. Liang L, Chen M, Duan L, *et al*. Research progress of thermal energy storage technology in solar thermal power generation and combined heat and power generation. Thermal Power Generation 2020; 49(3): 8–15.
9. Ji J, He Y. Strategic research on basic theory and key technology of solar thermal power generation system. Bulletin of National Natural Science Foundation of China 2009; 23(6): 331–336.
10. Yang C, Wang X, Zhang C, *et al*. Performances of gas turbine-based CCHP system combined with solar and compressed air energy storage. Proceedings of the CSEE 2017; 37(18): 5350–5358.
11. Li H, Nalim R, Haldi PA. Thermal-economic optimization of a distributed multi-generation energy system: A case study of Beijing. Applied Thermal Engineering 2006; 26(7): 709–719.
12. Zhang N, Cai R. Analytical solutions and typical characteristics of part-load performances of single shaft gas turbine and its cogeneration. Energy Con-

version and Management 2002; 43: 1323–1337.
13. Wang S, Fu Z, Xu L, *et al*. Analysis on typical daily hourly thermodynamic characteristics of integrated solar combined cycle system. Thermal Power Generation 2020; 49(3): 16–22.
14. Dudley VE, Koib GJ, Mahoney AR, *et al*. Test results SEGS LS-2 solar collector SAND 94-1884. New Mexico: Sandia National Laboratories; 1994. p. 15.
15. Montes MJ, Abanades A, Martinez-Val JM, *et al*. Solar multiple optimizations for a solar-only thermal power plant, using oil as heat transfer fluid in the parabolic trough collectors. Solar Energy 2009; 83(12): 2165–2176.
16. Behar O, Khellaf A, Mohammedi K. A novel parabolic trough solar collector model—Validation with experimental data and comparison to engineering equation solver (EES). Energy Conversion and Management 2015; 106: 268–281.
17. Zhao L. Shuibeng xingneng quxian de jiexi biaoda fangfa (Chinese) [Analytical expression method of pump performance curve]. China Rural Water and Hydropower 1992; (9): 38–39.
18. Liang Z, Chen Y, Xiao X, *et al*. Analysis on characteristics of cooling, heating and power loads of three commercial buildings in Guangzhou. Building Science 2012; 28(8): 13–20.